

TENSILE AND SHEAR CRACKS BEHAVIOR UNDER PLANE STRAIN SMALL SCALE YIELDING

V.N. Shlyannikov¹

¹ Kazan State Power Engineering Institute, Krasnoselskaya Street, 51, Kazan, 420066, Russia

ABSTRACT

In order to evaluate the mechanical behavior around stationary small scale yielding crack tip for plane strain, the asymptotic governing equation and their boundary conditions are formulated by the light of fracture mechanisms. A total deformation theory of plasticity with a power-law hardening is employed. The analysis of the near-tip fields are obtained for both tensile and shear boundary conditions, the complete range of mixity parameter and different strain hardening levels. Details of the mixed-mode fracture under mixed-mode loading and change fracture mechanism are also given. It is established that the intersection area of separate curves in coordinates of mixity parameter M_p versus crack growth direction, corresponding to each (between two) dominating fracture mechanism, form small zone of the really mixed mode fracture. The position of this zone of a crack unstable equilibrium correspond to change of the leading fracture mechanism or to the determination of the mixed mode ratio at which the transition of the fracture mode occur. The numerical values of elastic-plastic parameters describing of transition zone are well agreed with experimental data found in the literature which show that all change in fracture mode take place at a relative constant value of mixity parameter. By means of numerical investigation of mixed-mode loading problems it is obtained that there is only one total relationship between mixity parameter M_p and numerical constant I_n for both fracture mechanisms.

INTRODUCTION

One of the important points is that, for a large number of mixed-mode crack growth problems of which we are aware, there are two fundamentally distinct classes of growth: maximum principal stress-dominated and shear-dominated. This is true regardless of whether we consider static or cyclic loading conditions. Another point is the intimate connection of the crack tip displacement concept to mixed-mode elastic-plastic fracture and fatigue processes. Several elastic-plastic finite element analyses [1-5] and experimental investigations [6-14] showed non-uniform deformation and damage fields near an initially smooth notch tip under mixed mode loading. Aoki *et al* [1] predict that two competing process zone may be associated with the crack tip; one process zone, dominated by tensile stress and the other dominated by shear stress. The side of the notch, dominated by tensile stress, blunts, while the other side, dominated by shear strains, sharpens. It was shown in [11-14] that the stable crack under mixed-mode loading conditions propagates either as a mode I crack approximately in the direction normal to the maximum tangential stresses or as a shear crack in the maximum strain direction. It is possible that material failure due to shear crack propagation in the direction of maximum shear strains would occur in the localized band of intense plastic strain (referred in [11] as “shear crack”). The highest tensile hydrostatic stress and notch-tip constraint always occur near the blunted

part of the notch. In this region the crack growth direction is normal to the maximum tensile stresses. This type of mixed-mode ductile fracture mechanism is referred in [11] as “tensile crack” growth. It is clear from the preceding discussion that there are two competing fracture mechanisms that are operative near the sharpened and blunted part of the notch respectively in a ductile material under mixed-mode loading. The dominant mechanism (between two) establishes the stable crack growth direction.

Shih [15] examined a line crack subjected to combined mode I and mode II loading using a “small scale yielding” analysis of an elastic-plastic body under plane strain conditions (i.e. extending the HRR-solution [16,17] on mode I fracture to the mixed mode case). He showed that two parameters, the J-integral and mixity parameter M_p , define completely the near-tip asymptotic stress field. The analysis was related only to the tensile crack fracture mechanism (boundary conditions) for small scale yielding. Shih did not, however, take into consideration the fracture mechanism associated with shear crack. Even if some attempts have been made recently, there are currently no analytical results that predict the critical applied mixed mode ratio characterizing the usually abrupt change in fracture mode.

All the above analytical and numerical analyses on the effect dominance fracture mechanism at mixed-mode loading focused on mode I boundary conditions. A similar investigation for both tensile and shear cracks in elastic-plastic solids has not been carried out in the literature. In this paper, steady-state stationary crack in elastic-plastic solids is simulated using dominant singularity solution governing the asymptotic behavior at the crack tip. The analysis of the near-tip fields follows the works of Rice and Rosengren, Hutchinson and Shih [15-17]. Our investigation is carried out within the framework of mixed-mode (combining modes I and II), plane strain, small scale yielding conditions.

PROBLEM FORMULATION AND SOLUTION

The dominant singularity solution for a cracked plate of a strain hardening material known as the HRR-singular field [16,17], was completed by the solution for the mixed-mode elastic-plastic stress distribution, corresponding only tensile fracture mechanism, presented by Shih [15]. According to these approaches, the dominant singularity governing the asymptotic behavior of the stresses at the crack tip has the form

$$\begin{aligned}\sigma_{ij} &= \sigma_0 K_M^p r^{-1/(n+1)} \tilde{\sigma}_{ij} \\ \sigma_e &= \sigma_0 K_M^p r^{-1/(n+1)} \tilde{\sigma}_e\end{aligned}\quad (1)$$

where σ_0 is the yield stress in simple tension, K_M^p is the plastic stress intensity factor, and M_p is the near-field mixity parameter [15]. The dimensionless functions $\tilde{\sigma}_{ij}$ and $\tilde{\sigma}_e$ depend only on the polar angle θ , M_p and n . In the above relation, α and n are the hardening parameters of the Ramberg-Osgood power-law. Under plane strain conditions, when the elastic strains are negligible and the dimensionless effective stress is related to the stress components and the Airy dimensionless stress function $\tilde{\phi}$

$$\tilde{\sigma}_e^2 = \frac{3}{4}(\tilde{\sigma}_{rr} - \tilde{\sigma}_{\theta\theta})^2 + 3\tilde{\sigma}_{r\theta}^2 \quad (2)$$

$$\text{where } \tilde{\sigma}_{rr} = s\tilde{\phi} + \frac{\partial^2 \tilde{\phi}}{\partial \theta^2}, \quad \tilde{\sigma}_{\theta\theta} = s(s-1)\tilde{\phi}, \quad \tilde{\sigma}_{r\theta} = (1-s)\frac{\partial \tilde{\phi}}{\partial \theta}, \quad s = \frac{2n+1}{n+1}$$

In the present work the fourth-order differential equation governing the dominant singularity derived from the compatibility equation has the following form with taking into account Eqn. 2

$$\left(\frac{d^2}{d\theta^2} - a_1 \right) \left[\tilde{\sigma}_e^{n-1} \left(a_2 \tilde{\phi} + \frac{d^2 \tilde{\phi}}{d\theta^2} \right) \right] + a_3 \frac{d}{d\theta} \left(\tilde{\sigma}_e^{n-1} \frac{d\tilde{\phi}}{d\theta} \right) = 0, \quad \text{where } \tilde{\sigma}_e^2 = \frac{3}{4} \left(a_2 \tilde{\phi} + \frac{d^2 \tilde{\phi}}{d\theta^2} \right)^2 + a_4 \left(\frac{d\tilde{\phi}}{d\theta} \right)^2,$$

$$a_1 = n(s-2)[n(s-2)+2], \quad a_2 = s(2-s), \quad a_3 = 4(s-1)[n(s-2)+1], \quad a_4 = 3(1-s)^2. \quad (3)$$

Boundary conditions

For the total mixed mode loading case stress-free boundary conditions require

$$\sigma_{\theta\theta}(r,\pm\pi) = \sigma_{r\theta}(r,\pm\pi) = 0 \quad \text{or} \quad \tilde{\phi}(\pm\pi) = \tilde{\phi}_1(\pm\pi) = 0 \quad (4)$$

$$\text{where} \quad \frac{d\tilde{\phi}}{d\theta} = \tilde{\phi}_1; \quad \frac{d\tilde{\phi}_1}{d\theta} = \tilde{\phi}_2; \quad \frac{d\tilde{\phi}_2}{d\theta} = \tilde{\phi}_3.$$

We propose to complete the boundary conditions for mixed mode loading proceeding from the assumption that the dominant fracture mechanism establishes the stable crack growth direction. Thus, the dimensionless stresses and strains, appropriate each fracture mechanism, has to have extremum along the crack growth direction $\theta = \theta^*$. For the case, dominated by tensile fracture mechanism, the crack growth direction is normal to the maximum tensile stress and then

$$\frac{d\tilde{\sigma}_{\theta\theta}(\theta^*)}{d\theta} = 0; \quad \tilde{\sigma}_{r\theta}(\theta^*) = 0; \quad \tilde{\phi}_1(\theta^*) = 0 \quad \text{for} \quad -\pi/2 < \theta^* < 0. \quad (5)$$

In the case of the shear dominant fracture mechanism crack growth in the direction of maximum shear strain (stress). Thus we have to satisfy the following conditions

$$\frac{d\tilde{\sigma}_{r\theta}(\theta^*)}{d\theta} = 0; \quad \tilde{\phi}_2(\theta^*) = 0 \quad \text{for} \quad -\pi/2 < \theta^* < 0. \quad (6)$$

Finally, the nonlinear compatibility equation 3 for plane strain small scale yielding was solved numerically using an iteration scheme taking into account the above boundary conditions (Eqns.4-6). Our analytical results concerning the dimensionless stresses distributions for tensile fracture boundary conditions under plane strain, in general, confirm the study of Shih [15]. Unlike the investigation of Shih [15], in the present paper, the near-field mixity parameter, M_p , was obtained directly from both $\tilde{\sigma}_{\theta\theta}$ and $\tilde{\sigma}_{r\theta}$ θ -distributions. For shear fracture boundary conditions new results were obtained whose details are given in Figs.1-3. In mixed mode small-scale yielding, the plastic stress intensity factor K_M^p in Eqn.1 is related to the numerical value of the definite integral $I_n(M_p)$ that depends on the fracture angle θ^* , the strain-hardening exponent n and the mixity parameter M_p

$$I_n(\theta^*, M_p, n) = \int_{-\pi}^{\pi} \Omega(n, \theta) d\theta \quad (7)$$

where

$$\begin{aligned} \Omega(n, \theta) &= \frac{n}{n+1} \tilde{\sigma}_e^{n+1} \cos\theta - \left[\tilde{\sigma}_{rr} \cdot \left(\tilde{u}_\theta - \frac{d\tilde{u}_r}{d\theta} \right) - \tilde{\sigma}_{r\theta} \cdot \left(\tilde{u}_r + \frac{d\tilde{u}_\theta}{d\theta} \right) \right] \sin\theta - \frac{1}{n+1} (\tilde{\sigma}_{rr} \tilde{u}_r + \tilde{\sigma}_{r\theta} \cdot \tilde{u}_\theta) \cos\theta \\ \tilde{u}_r(\theta) &= \frac{3}{4} (n+1) \tilde{\sigma}_e^{n-1} [a_2 \tilde{\phi} + \tilde{\phi}_2]; \quad \frac{d\tilde{u}_r}{d\theta} = \frac{3(n+1)}{4} \tilde{\sigma}_e^{n-3} \left[\frac{n-1}{2} \cdot \phi_1 \cdot (a_2 \tilde{\phi} + \tilde{\phi}_2) + \tilde{\sigma}_e^2 (a_2 \tilde{\phi}_1 + \tilde{\phi}_3) \right] \\ \tilde{u}_\theta &= \frac{n+1}{n} \left[\frac{d\tilde{u}_r}{d\theta} - 3\tilde{\sigma}_e^{n-1} (1-s) \cdot \tilde{\phi}_1 \right]; \quad \tilde{u}_\theta - \frac{d\tilde{u}_r}{d\theta} = \frac{1}{n} \frac{d\tilde{u}_r}{d\theta} - 3 \frac{n+1}{n} \tilde{\sigma}_e^{n-1} (1-s) \tilde{\phi}_1; \quad \tilde{u}_r + \frac{d\tilde{u}_\theta}{d\theta} = (s-2) \tilde{u}_r. \\ \phi_1 &= \frac{3}{2} (a_2 \tilde{\phi} + \tilde{\phi}_2) (a_2 \tilde{\phi}_1 + \tilde{\phi}_3) + 2a_4 \cdot \tilde{\phi}_1 \cdot \tilde{\phi}_2 \end{aligned}$$

Values of $I_n(\theta^*, M_p, n)$ are calculated for both fracture mechanism, i.e. for the tensile boundary conditions and the shear one when n changes from 2 to 13 and M_p changes from 0 up to 1.

RESULTS AND DISCUSSION

In this work full range of mixed mode loadings from pure mode I up to pure mode II are studied for materials with $n = 2, 3, 5, 9$ and 13 . The mode mixity parameter M_p and the definite integral I_n related to plastic stress intensity factor K_M^p was evaluated from two sets of elastic-plastic fields, one being the tensile crack behavior field and another the shear crack behavior field. Strain hardening plasticity solutions for small-scale yielding crack problems in plane strain by Eqns.3-6 are used for two competing fracture mechanisms that are operative near a crack tip in a ductile material under mixed mode loading. The typical θ -variations of the dimensionless stresses $\tilde{\sigma}_{ij}$ and the effective stress $\tilde{\sigma}_e$ are shown for both type of boundary conditions in Fig.1. Results are displayed in these figures corresponding approximately to identical values of the mode mixity parameter M_p for each fracture mechanism. It must be noted that the near-tip angular elastic-plastic stresses variations for the tensile crack and the shear crack are different. Furthermore, it can be seen from Fig.1 that angular position of θ^* which determines crack growth direction are different for the same value of M_p for both types of boundary conditions. The angular variations of dimensionless tangential stress $\tilde{\sigma}_{\theta\theta}$ and shear strain $\tilde{\epsilon}_{r\theta}$ are shown in Fig.2 for $n=3$ and $n=13$. These distributions corresponding to full range of near-tip mixity parameter M_p . The position of a maximum on each curve determines of the crack growth direction within the limits of the examined fracture mechanism. As already mentioned, maximum of tangential stress $\tilde{\sigma}_{\theta\theta}$ corresponds to the tensile crack boundary conditions, while maximum of shear strain $\tilde{\epsilon}_{r\theta}$ describes shear crack behavior. It is clear from our study that the direction of crack extension under mixed mode loading is strongly dependent upon the dominant fracture mechanism and work hardening characteristics of the material.

The dependences between the near-tip mixity parameter and the definite integral for both type of boundary conditions are presented in Fig.3,a. Interestingly, as it follows from this figure, for each strain hardening exponent n there is one total relationship between mixity parameter M_p and numerical constant I_n for both fracture mechanisms. It confirms existence of one common elastic-plastic stress intensity factor K_M^p in contrast an elastic situation when take place a superposition of two separate stress intensity factors K_I and K_{II} .

The crack angle θ^* that determines of crack growth direction is function of the fracture mechanism, the power hardening coefficient n and mixity parameter M_p . Figure 3,b show, respectively, variations of θ^* with respect to n and M_p . It must be noted that, in general case, under mixed mode loading there are not mixed mode fracture. The stable crack under mixed mode loading conditions propagates only either as a tensile crack approximately in the direction normal to the maximum tangential stresses or only as a shear crack in the maximum shear strain direction. As it follows from Fig.3,b the intersection area of separate curves in coordinates of mixity parameter M_p versus crack growth direction θ^* , corresponding to each (between two) dominating fracture mechanism, form small zone of the really mixed mode fracture. The position of this zone of a crack unstable equilibrium correspond to change of the leading fracture mechanism or, in other words, to the determination of the mixed mode ratio at which the transition of the fracture mode occur. So, the change of the dominant fracture mechanism occurs in a range of values elastic mixity parameter $M_e=0.65\div 0.72$ or corresponding values of plastic mixity parameter $M_p=0.75\div 0.78$ at $\theta^*=35^\circ\div 40^\circ$. The found numerical values of elastic-plastic parameters describing of transition zone are well agreed with experimental data for the ferritic steels [12] which show that all change in fracture mode take place at a relative constant value of mixity parameter $M_e=0.68$. The dependences of the definite integral I_n on crack growth direction angle θ^* are presented in Fig.3,c.

CONCLUSIONS

The fact that dominant fracture mechanism (between two) establishes the stable crack growth direction was analyzed and discussed. It is assumed that under mixed mode loading shear crack propagation would occur in a sharpens side of the notch tip while crack growth normal to the maximum tensile stresses occur near the blunted part of the notch. From this point of view, nonlinear analysis has been made by solving the

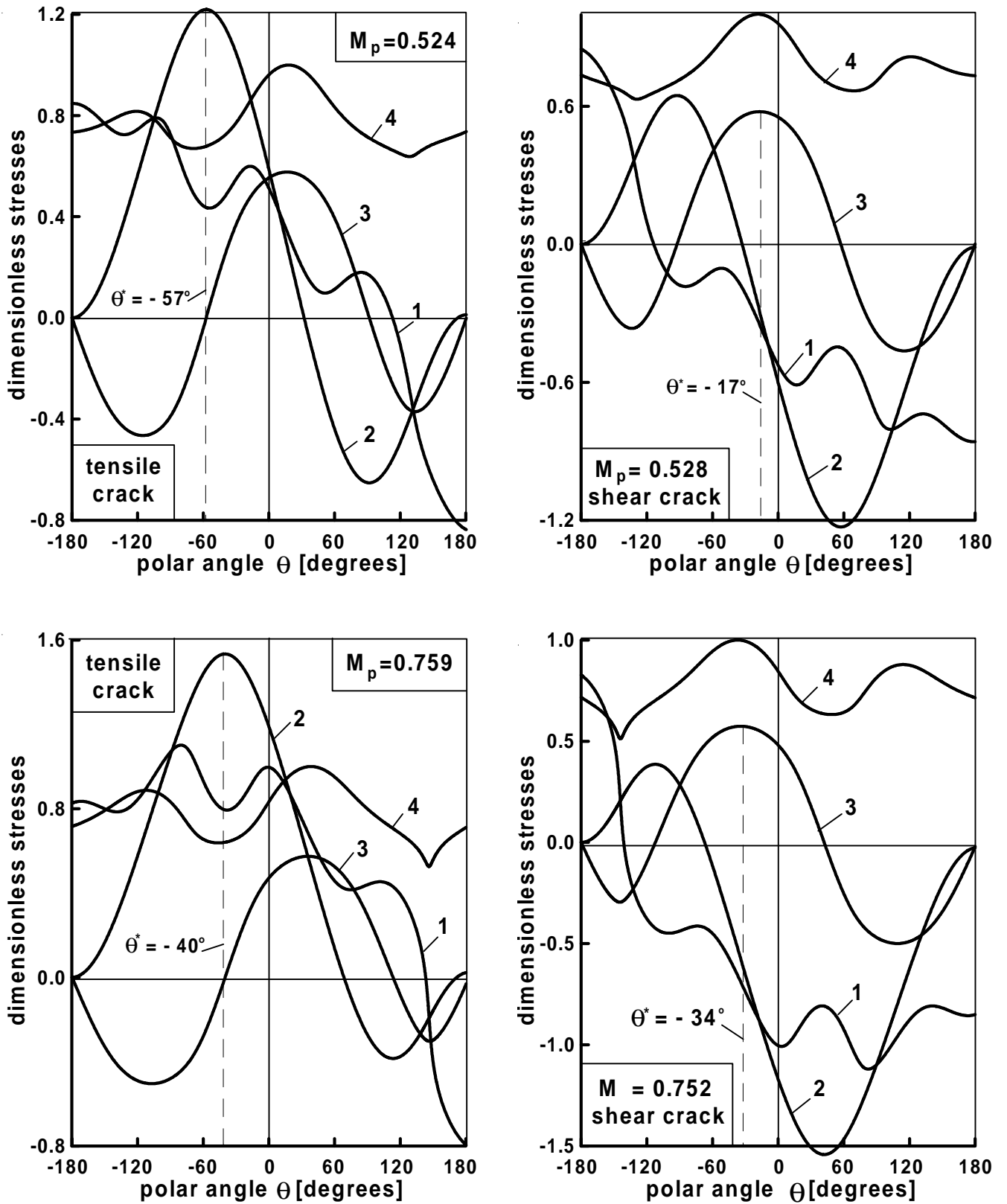


Figure 1: Angular stress distributions for different mode-mixity M_p corresponding to strain hardening $n=5$
 1 - $\tilde{\sigma}_{rr}$, 2 - $\tilde{\sigma}_{\theta\theta}$, 3 - $\tilde{\sigma}_{r\theta}$, 4 - $\tilde{\sigma}_e$

partial differential equations governing the dominant singularity to study the deformation, stress and strain near the crack tip under mixed mode plane strain loading conditions. In the present work was completed the boundary conditions for compatibility equation proceeding from the assumption that the stresses have

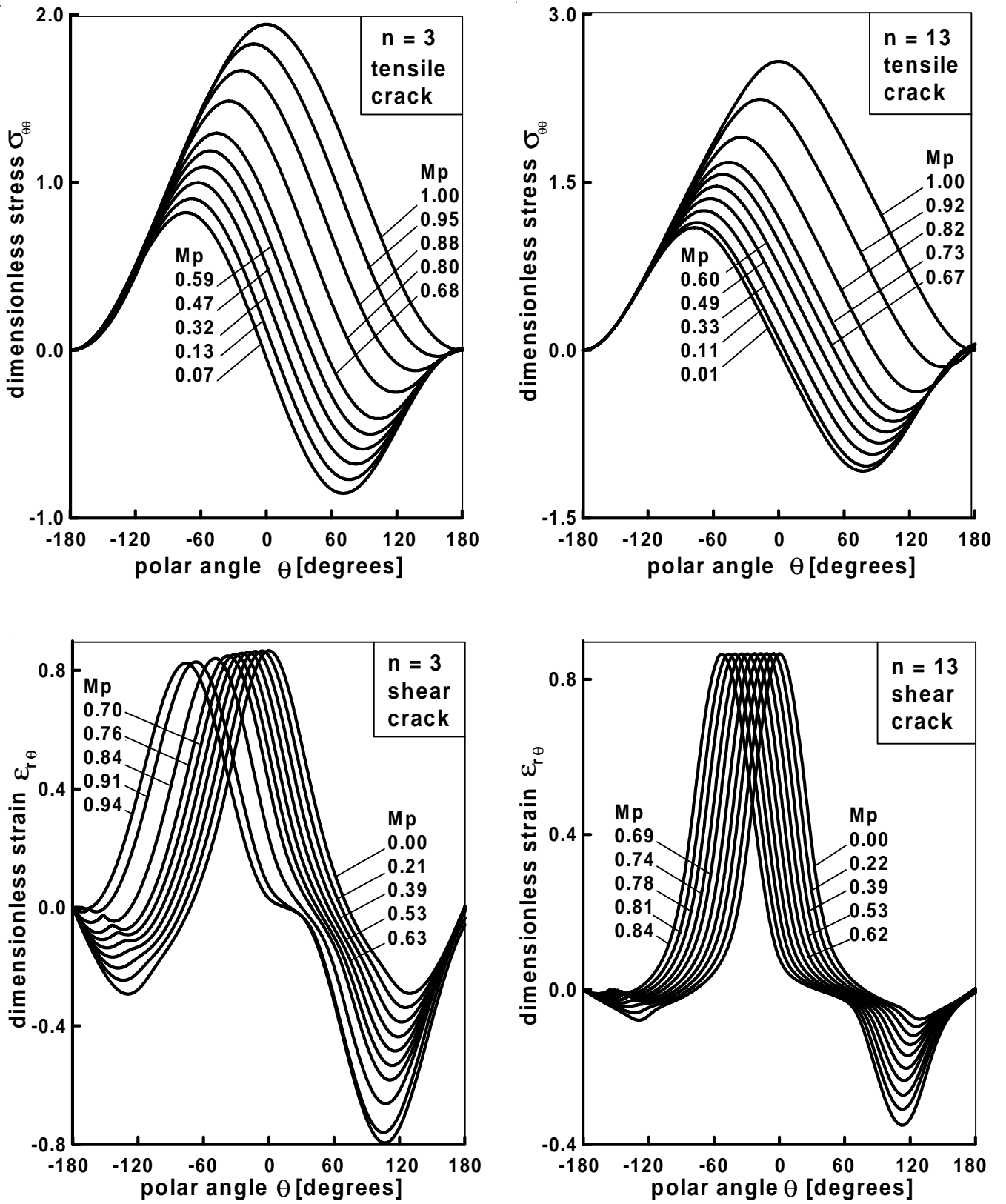


Figure 2: Variations of tangential stress and shear strain for different near-tip mixities corresponding to $n=3$ and $n=13$

to have extremum along the crack growth direction. Corresponding each dominant fracture mechanism near crack tip stress and strain fields are obtained for the complete range of mixed mode loading between Mode I and Mode II. By means of numerical investigation of mixed mode loading problems it is obtained

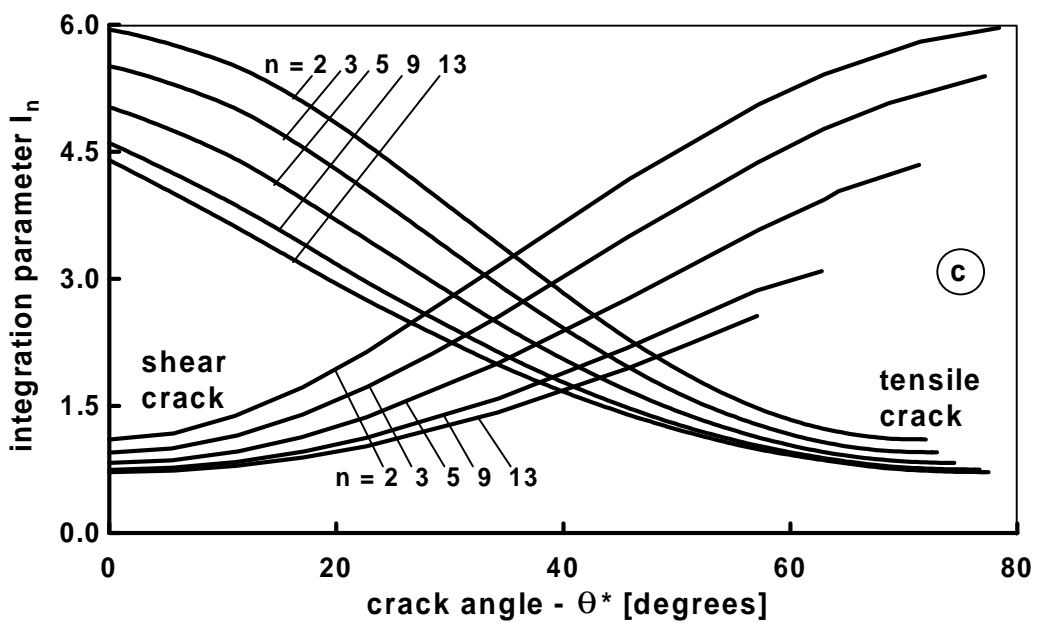
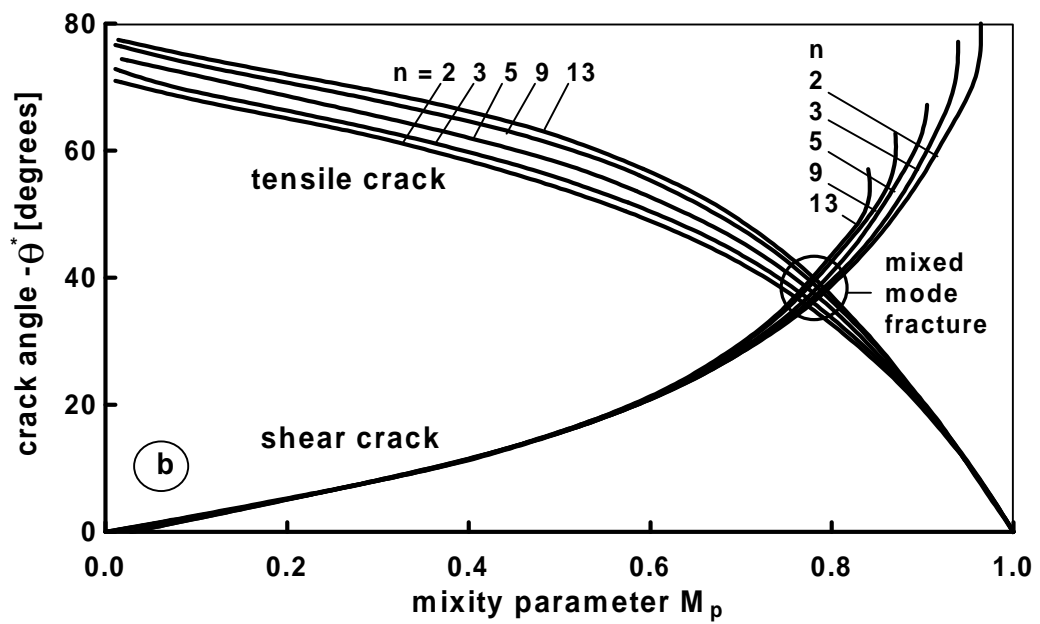
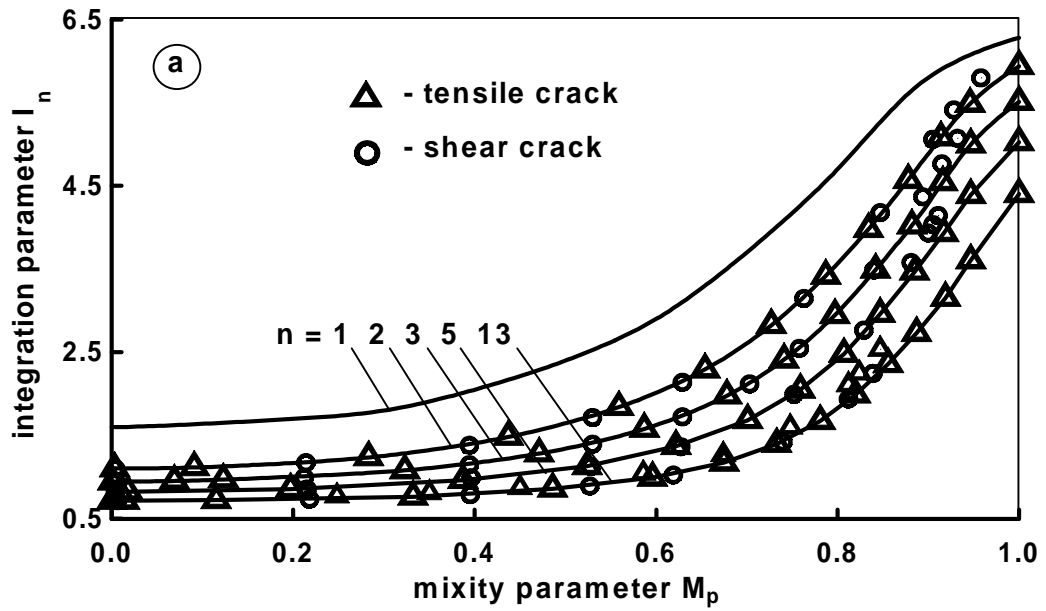


Figure 3: Integration parameter I_n and crack angle θ^* as functions of near-tip mode-mixity M_p

that there is only one total relationship between mixity parameter M_p and numerical constant I_n for both fracture mechanisms. It is established that the intersection area of separate curves in coordinates of mixity parameter M_p versus crack growth direction, corresponding to each (between two) dominating fracture mechanism, form small zone of the really mixed mode fracture. The position of this zone of a crack unstable equilibrium correspond to change of the leading fracture mechanism.

REFERENCES

1. Aoki S., Kishimoto K., Yoshida T., Sakata M.(1987) *J. Mech. Phys. Solids* **35**, 431.
2. Dhirendra V.K., Narasimhan R. (1998) *Engng. Fract. Mech.* **59**, 543.
3. Arun Roy Y., Narasimhan R.(1999) *Int. J. Solids Struct.* **36**, 1427.
4. Li J. (1998) *Engng. Fract. Mech.* **61**, 355.
5. Xiaosheng Gao, Shih C.F. (1998) *Engng. Fract. Mech.* **60**, 407.
6. Miller K.J., Brown M.W., Yates J.R. (1999) *ASTM STP 1359*, 229.
7. Shlyannikov V.N. (1996) *Theoret. Appl. Fract. Mech.* **25**, 187.
8. Maccagno T.M., Knott J.F. (1991) *Engng. Fract. Mech.* **38**, 111.
9. Bhattacharjee D., Knott J.F. (1994) *Acta Metall. Mater.* **42**, 1747.
10. Shlyannikov V.N. (1999) *ASTM STP 1359*, 279.
11. Dalle Donne C., Doker H. (1997) *ASTM STP 1280*, 243.
12. Dalle Donne C.(1999) *ASTM STP 1359*, 21.
13. Laukkanen A., Wallin K., Rintamaa R.(1999) *ASTM STP 1359*, 3.
14. Chao Y.-J., Zhu X.-K.(1999) *ASTM STP 1359*, 41.
15. Shih C.F. (1974) *ASTM STP 560*, 187.
16. Hutchinson J.W. (1968) *J. Mech. Phys. Solids* **16**, 13.
17. Rice J.R., Rosengren G.F. (1968) *J. Mech. Phys. Solids* **16**, 1.